

SIMULATION OF A HYPERSONIC FLOW OVER VEHICLES AT LOW REYNOLDS NUMBERS

V. N. Gusev
 Central Aerohydrodynamic Institute
 Zhukovsky, Moscow Region, Russia

Abstract

Some relationships between similarity criteria used and reasoning for their specific application in different combinations when simulating hypersonic gas flows from continuum to free-molecular ones are established on the basis of an analytical investigation. The possibilities of using current numerical analysis in the problems of the simulation and determination of aerodynamic and thermal characteristics of hypersonic vehicles in full-scale conditions are considered. The problem of a local simulation is discussed in connection with experimental investigations of local flow peculiarities that cannot be revealed during the simulation of hypersonic flows as a whole. Near the body surface in flow it is reduced to a respective problem of a subsonic viscous gas body surface flow with a given vorticity distribution. In the experiment this condition can be provided by using porous media.

The paper presents major variation laws for aerodynamic and thermal characteristics of hypersonic vehicles and their components under varying main similarity criteria. The experimental and computed results obtained are analyzed and summarized, they are compared with flight test data.

Nomenclature

- C_i - aerodynamic characteristic coefficient;
- C_D - drag coefficient;
- C_L - lift coefficient;
- C_M - pitching moment coefficient;
- $C = (\mu_{*T_*}) / (\mu_{\infty T_{\infty}})$;
- D - recess diameter or groove width;
- d - recess or groove depth;
- $F(\Delta) = (C_i - C_i^{\infty}) / (C_i^0 - C_i^{\infty})$;
- $\vec{g} = \vec{c}_{\infty} - \vec{c}_w$;
- H - flight altitude;
- h - enthalpy;
- K - lift-to-drag coefficient;
- K_w - atom recombination rate;
- Kn - Knudsen number;
- L - characteristic body dimension;
- M - Mach number;
- n - power in $\mu \propto T^n$;
- Pr - Prandtl number;
- p - pressure;
- q_i - parameters characterizing air composition and state;
- Re - Reynolds number;
- r_i - parameters characterizing surface properties;
- Sc - Schmidt number;
- St - Stanton number;
- T - temperature;

- $t_w = T_w / T_0$;
- U - velocity;
- $\overline{V_{\infty}} = M_{\infty} / \sqrt{C / Re_{\infty}}$;
- x - coordinate along the body;
- α - angle of attack;
- β_i - accommodation coefficients;
- δ - boundary layer thickness;
- $\epsilon = M_{\infty}^n / \sqrt{Re_{\infty}}$;
- ζ - Danköeler number;
- $\vec{\xi}$ - molecule velocity vector;
- ρ - density;
- λ - molecular free path;
- μ - viscosity coefficient;
- τ_i - characteristic relaxation time;
- σ - molecule collision section;
- Ω_i - parameters characterizing air transport properties.

Subscripts:

- ∞ - undisturbed flow;
- w - surface values;
- 0 - stagnation parameters;
- i - component;
- $*$ - characteristic parameter values.

Superscripts:

- ∞ - continuum values;
- 0 - free-molecular values.

Introduction

The simulation conditions of hypersonic flows over vehicles from continuum to free-molecular ones include an equality of a great number of dimensional and non-dimensional parameters characterizing physical and chemical processes in gas, its state in an undisturbed flow and on the body surface. In the general case the simulation of such flows is possible only for a full coincidence of flow conditions, i.e. in case of an equality of the whole combination of governing parameters:

$$\alpha, \rho_{\infty}, P_{\infty}, h_{\infty}, h_w, U_{\infty}, L, q_{i\infty}, r_{i\infty}, \Omega_i, \tau_i.$$

It is impossible to fully simulate a hypersonic flight of a vehicle with respect to all above listed parameters in current wind tunnels. In this case it is reasonable to resort to a partial simulation when it becomes possible to take advantage of similarity laws formulated in different flow regions.

The characteristic relaxation times τ_i of such energy-consuming processes as dissociation, chemical reactions and ionization absorbing more than

75% of the flow energy will be considerably greater than the characteristic gasdynamic time L/U_∞

at low Reynolds numbers because of the shock wave merging and the cooled body surface influence. In this case the air composition in the disturbed flow region near the body surface will be close to the frozen composition ($q_i = \text{const}$). In these conditions non-equilibrium physical-chemical processes in air are taken into account with respect to oscillatory, rotational and translational degrees of freedom of molecules. But because of small amount of energy in internal molecule degrees of freedom, its contribution to the transfer of flow momentum and energy to a surface element will be insignificant. Only in case of the flow pattern near the body this effect may become significant.

In these conditions, the simulation problem is simplified, since the similarity laws for a thermodynamically perfect gas become valid in the assumed statement. However, a full wind tunnel simulation of vehicle flight conditions at low Reynolds numbers also remains a very difficult problem in this case. Additional information is required that establishes the dependence of sought nondimensional parameters on the similarity criteria that are different in wind tunnels and in real flight conditions.

Simulation of Hypersonic Flows With Frozen Air Composition.

In the general case, the similarity conditions, following from the dimensional theory, for a stationary thermodynamically perfect gas flow with given infinity parameters over bodies include body geometry similarity and equality of the following similarity criteria:

$$\alpha, M_\infty, Re_\infty, Pr, Sc, \zeta_w, t_w, \Omega_i, \beta_i. \quad (1)$$

The Knudsen number may enter into (1) instead of Re_∞ :

$$Kn \approx \lambda_\infty / L \approx M_\infty / Re_\infty.$$

In case of an infinite increase in the Mach number M_∞ the similarity criteria system (1) should be modified since temperature T_∞ in this case becomes insignificant and falls out of the system of governing parameters. At infinity, $\rho_\infty U_\infty$ will remain among these parameters and the characteristic temperature is determined in terms of stagnation temperature $T_0 \approx U_\infty^2$. The Reynolds number $Re_0 = \rho_\infty U_\infty L / \mu(T_0)$ will enter, instead of Re_∞ , into the similarity criteria corresponding to these dimensional parameters in the hypersonic stabilization condition at $M_\infty \rightarrow \infty$.

Note here that the criterion $Re_w = \rho_\infty U_\infty / \mu_w(T_w)$ that for power dependence $\mu \approx T^n$ is equal to

$$Re_w = Re_0 \frac{\mu_0}{\mu_w} = t_w^{-n} Re_0$$

follows from the same system of governing parameters.

As for an ideal gas, the flow independence of Mach number at $M_\infty \gg 1$ is attributed to freezing of the undisturbed flow field in front of the body past a strong shock wave when $T_\infty \rightarrow 0$. In the other limiting case of a free-molecular flow the hypersonic stabilization principle follows from an immediate consideration of the expressions for local values of momentum and energy transferred to an element surface.

In the description of hypersonic viscous gas flows the principle of the flow independence of M_∞ remains also valid in the presence of the boundary layer. This principle for a flow over slender pointed bodies was indicated in [1]. In case of blunt bodies for which the flow independence of Mach number is already fulfilled at comparatively low supersonic velocities the similarity parameter ϵ used in numerous papers is unambiguously related to the criterion Re_0 :

$$\epsilon = M_\infty^n / \sqrt[4]{Re_\infty} \approx Re_0^{-1/2}$$

The same parameter is also characteristic of such secondary effects in the boundary layer as gas slip and temperature jump on the body surface.

As for very blunt bodies, the Reynolds number $Re_2 = \rho_2 U_2 / \mu_2$ based on flow parameters behind the shock wave front is often used in a number of papers for the correlation of experimental data. The application of this criterion can be reasonable for taking account of physical-chemical processes in air at high flight velocities. For a thermodynamically perfect gas with an accuracy of several per cents the criterion is as follows:

$$Re_2 = \rho_2 U_2 L / \mu_2 = \rho_\infty U_\infty L / \mu_2 \approx Re_0$$

Similarity conditions for hypersonic flows in the transition region lying between continuum and free-molecular flow conditions were formulated in [2]. The analysis made in this paper indicated the conditions at which the criterion Re_0 is a strict consequence of the Boltzmann equation.

The validity of using the similarity criteria including Re_0 in the hypersonic stabilization conditions is confirmed by many experimental and numerical data on aerodynamic and thermal characteristics of a wide class of bodies (see, e.g., [3]). In a number of cases the application of the criterion Re_0 allows the results to be correlated not only for varying Mach numbers, M_∞ but also other varying similarity criteria. In addition, at $U_\infty = \text{const}$ it follows from the condition that $Re_0 = \text{const}$ that the law of binary similarity $\rho_\infty L = \text{const}$ is fulfilled when simulating nonequilibrium flows.

In order to exclude other similarity criteria in the correlation of experimental and computation

data use is made of the parameters that are combinations of initial parameters. Those can, e.g., be the interaction parameter $\bar{V}_\infty = M_\infty / \sqrt{C/Re_\infty}$ that is widely applied. Physically, this parameter characterizes the quantity proportional the ratio of molecular free path λ in an undisturbed flow to characteristic boundary layer thickness δ :

$$\frac{\lambda_\infty}{L} \sim \frac{M_\infty}{Re_\infty}; \quad \frac{\delta}{L} \sim Re_\infty^{-1/2} \rightarrow \frac{\lambda_\infty}{\delta} \sim \frac{M_\infty}{\sqrt{Re_\infty}} \sim \bar{V}_\infty.$$

At $T_x = T_0$, we have $\bar{V}_\infty = Re_0^{-1/2}$. Even more complex expressions for characteristic temperature T_x are used in practice.

In a region adjacent to a free-molecular one, the free path of molecules reflected from the body relative to incident molecules $\lambda_{w\infty}$ is governing among characteristic molecular free paths [4]. The Knudsen number based on this path is:

$$Kn_{w\infty} = \frac{\lambda_{w\infty}}{L} \approx \frac{|\vec{\xi}_w|}{\rho_\infty \sigma |g| L}.$$

Consequently:

$$Kn_{w\infty} \sim \frac{\sqrt{T_w}}{\rho_\infty \sigma (T_0) U_\infty L} \sim \frac{t_w^{1/2}}{\rho_\infty \sigma (T_0) L} \sim t_w^{1/2} Kn_\infty \frac{\sigma(T_\infty)}{\sigma(T_0)}$$

and independent of the collision section variation law:

$$Kn_{w\infty} \approx t_w^{1/2} Re_0^{-1}$$

Obviously, the validity of applying similarity criterion combinations is justified when the influence of individual similarity criteria on the final result disappears. Alongside with the above functional dependencies following from similarity laws, wide use is made for this purpose of numerous experimental data obtained in hypersonic, shock, impulse and vacuum wind tunnels, as well as of numerical experiment. In case of a continuum flow, the viscous effect on aerodynamic characteristics is caused primarily by surface friction and additional pressure induced by a displacing action of the boundary layer (so-called hypersonic viscous interaction condition). The calculation procedure of local values of pressure, friction and heat transfer coefficients over a wide range of similarity parameters variation in this condition is presented most fully in [5]. At present, numerical solutions of the Navier-Stokes, Boltzmann equations and their asymptotic models [3] are used successfully in the transition region. The possibilities of the application of this entire information in the simulation and determination of aerodynamic and thermal characteristics of hypersonic vehicles in full-scale conditions are discussed below.

Correlation of Aerodynamic and Thermal Characteristics and Their Scaling for Real Conditions.

At present, the correlation of some aerodynamic characteristics at hypersonic stabilization conditions is reduced to one-parameter dependencies. For example, for such a characteristic as body

drag the dependence $F = (C_D - C_D^\infty) / (C_D^0 - C_D^\infty)$ on parameter $\Delta = t_w^{0,1} Re_{0x} \sin \alpha_x$ which is normalized with respect to limiting values proved to be common for a wide class of nonsimilar bodies [6]. The correlation dependence for this characteristic

$$F(\Delta) = \begin{cases} 0,7 \exp[-0,57(\lg \Delta) - 0,228(\lg \Delta)^2] & \text{at } \lg \Delta \geq -1,25 \\ 1 & \text{at } \lg \Delta < -1,25 \end{cases}$$

obtained by using numerous experimental and computation data is shown in fig.1.

The application of the dependence $F(\Delta)$ for the determination of full-scale values of C_D presupposes the knowledge of limiting values of C_D^∞ and C_D^0 . In a continuum flow, the values of C_D^∞ can be obtained by using the Euler equations or as a result of wind tunnel tests. Free-molecular values of C_D^0 are obtained in numerical integration of local aerodynamic characteristics of surface elements. For particular coatings, the latter are found using the results of the experiments conducted in the facilities "molecular source".

In some cases, function $F(\Delta)$, obtained for drag coefficient C_D , retains its form in the calculation of other aerodynamic characteristics. For the

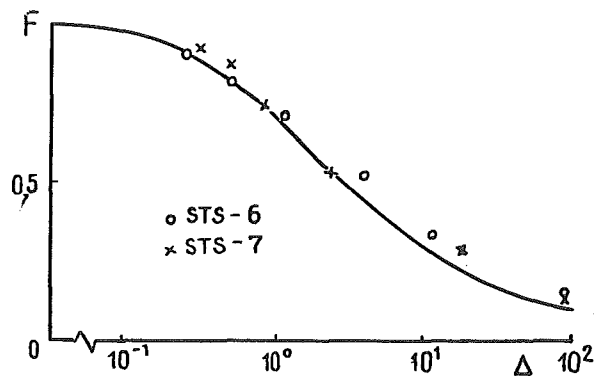


Figure 1. The Body Drag Correlation Dependence.

coefficients of lift and pitching moment of simple bodies it is confirmed by the comparative analysis results in [6]. The values of $F(\Delta)$ computed for the axis force coefficient of Space Shuttle in real conditions [7] are in sufficiently good agreement with the correlation dependence $F(\Delta)$ and given in Fig.1.

The above procedure of the determination of full-scale values of aerodynamic characteristics was tested in real flights. The values of the lift-to-drag ratio K in Fig.2 obtained for one of flying models using this procedure are compared with the flight test results [8]. This figure also presents a similar comparison for Space Shuttle [9]. Agreement between predicted and flight data is quite satisfactory. As for the errors in this figure, their level in a free-molecular region is essentially attributed to uncertainty in gas molecule - surface interaction laws. For example, the error in the determination of lift in laboratory conditions for test specimens of one and the same material amount to $\pm 60\%$. In scaling

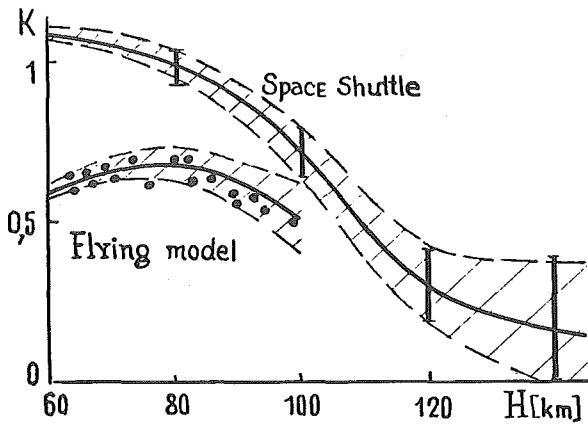


Figure 2. Comparison of Predicted and Flight Lift-To-Drag Ratio Data.

for the real flight conditions it increases exceeding the value to be measured.

The technique of the determination of full-scale aerodynamic characteristics of hypersonic vehicles from continuum to free-molecular flow conditions was used during the development and construction of the aerospace plane Buran. As an example for pitching moment it is illustrated in Fig.3 by the dependence of C_m on angle of attack α at $M_\infty = 28$ and altitude $H = 90$ km [10]. This figure

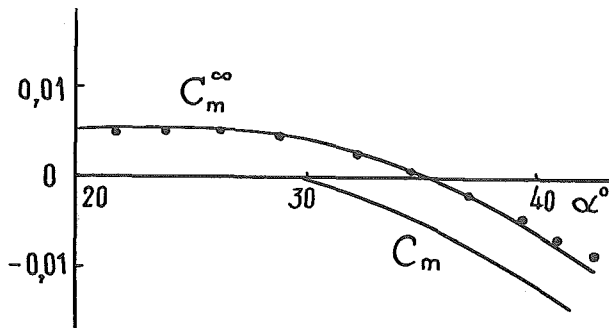


Figure 3. Comparison of Predicted and Buran Flight Test Data for Pitching Moment Coefficient

also shows predicted and experimental values of C_m^∞ corresponding to inviscid flow over the vehicle at $M_\infty = 10$. Viscosity and rarefaction result in a reduction in pitching moment and trim angle of attack. In the flight test, this effect was recorded for one of flying models.

In a flow over relatively slender bodies at low angles of attack, when the principle of the flow independence of the Mach number, M_∞ , is violated, some aerodynamic characteristics in transition region may vary nonmonotonically. The existence of such flow conditions was confirmed repeatedly by experimental and numerical investigations (see, e.g., [3]). In these cases, it is reasonable to represent the aerodynamic characteristic C_i as the following sum:

$$C_i = [F(\Delta)(C_i^D - C_i^\infty) + C_i^\infty] + C_{ix}$$

where $F(\Delta)$ is the above found function, while the nonmonotone component C_{ix} is given in [11] based on processing of systematic calculated and experimental results for various bodies.

Fig.4 represents the dependence of lift coefficient C_L on Reynolds number Re_0 at $\alpha = 20^\circ$, $M_\infty = 8$, $t_w = 1$ obtained by using this technique for one of schematized models of a hypersonic vehicle as a slender pointed semicone with a delta wing. Its agreement with accurate computed and experimental values given in the figure is quite satisfactory.

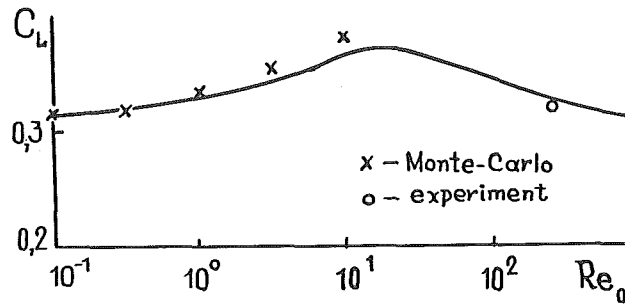


Figure 4. The Dependence of Lift Coefficient on Reynolds Number for Schematized Hypersonic Vehicle

The application of similarity criteria, including Reynolds number Re_0 , for hypersonic stabilization conditions simplifies considerably the problem of the determination of temperature distribution over the hypersonic vehicle surface. At $Re_0 = const$ the influence of individual similarity criteria that have different values in a wind tunnel and in real conditions on local values of the heat flux along body generatrix x becomes insignificant away from the critical point. This is indicated, e.g., by the results of a numerical calculation of the Navier-Stokes equations and experimental data for a hyperboloid [12] shown in Fig.5. The difference between real ($M_\infty = 20$, $t_w = 0,02$) and wind tunnel ($M_\infty = 6,5$, $t_w = 0,3$) Stanton numbers, $St(x)$, for the selected similarity criteria amounts to several per cents at high values of x . In this case, the relative distribution of heat fluxes over the body surface $St(x)/St(0)$ will be the same everywhere at high values of Re_0 , when $St(0) \approx Re_0^{-1/2}$.

Local Simulation of Hypersonic Flows.

In experimental investigations of local flow peculiarities that cannot be revealed in the simulation of a flow as a whole, local simulation problems gain greatly in importance. It refers, first of all, to such heat-stressed hypersonic vehicle components as its nose tip and wing leading edges.

The functional dependences from continuum to free-molecular flow conditions for heat fluxes to these components obtained on the basis of numerous experimental and computed results are presently reduced to simple approximation dependences (see, e.g., [13]). For the stagnation point they are

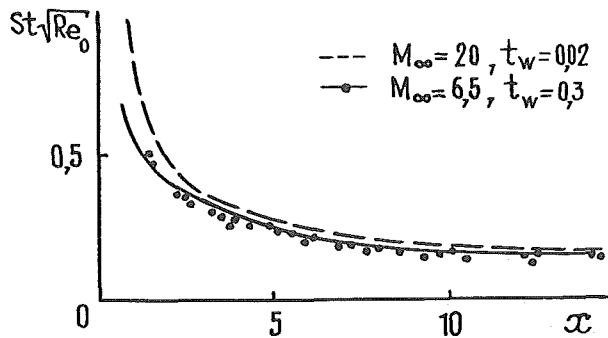


Figure 5. Heat Flux Distribution Over Hyperboloid.

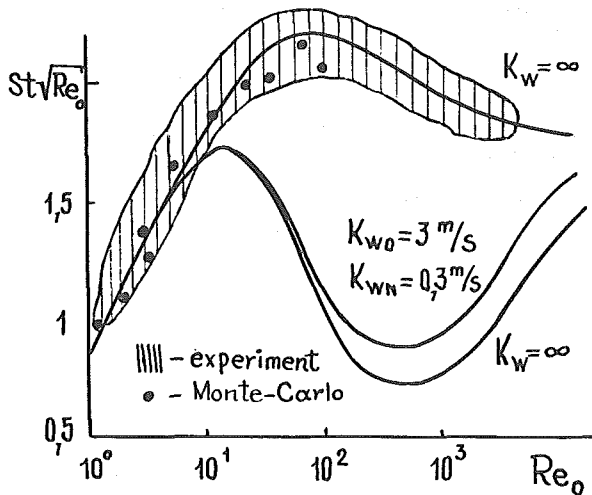


Figure 6. Stagnation Point Heat Flux

given in Fig.6. As for the circular velocity in case of an ideally catalytic surface ($K_V = \infty$), the influence of nonequilibrium processes on heat transfer in transition region is relatively small. Here, the nonequilibrium values of Stanton number St are close to the values that correspond to the frozen case.

Of more importance in heat transfer problems at low Reynolds numbers become the phenomena occurring on the body surface. Slip effects become great enough, especially at temperature factor $t_V = O(1)$. The phenomena associated with noncatalytic surface properties have an even greater influence on temperature. In this case, atom recombination rates K_V obtained in laboratory conditions are used in the definition of temperature distribution over the vehicle surface with final catalyticity as boundary conditions for the Navier-Stokes equations. The results of such computations in the vicinity of the stagnation point of Buran taken from [8] are given in fig.7. The thermal coating temperature of the Buran nosetip at nitrogen and oxygen atom recombination rates $K_V = 2$ m/s experimentally measured in laboratory conditions proves to be 300° lower than for an ideally catalytic surface ($K_V = \infty$).

Impinging shock - bow shock wave interference leads to a considerable increase in heat transfer

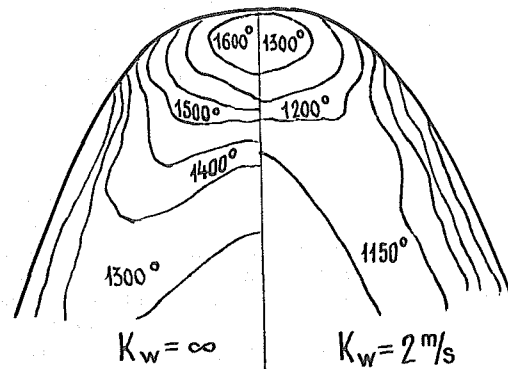


Figure 7. Temperature Distribution Over Buran Nosetip Region [8].

to hypersonic vehicle edges. A local simulation of this phenomenon for a laminar flow condition and relatively high Reynolds numbers shows that, in accord with the adopted classification, the greatest rise in heat transfer takes place in type IV interference case, when an oblique shock impinges on a bow shock wave section that is normal to free stream velocity vector. Fig.8 [14] presents experimental values of a maximum increase in heat transfer $\overline{St}_{max} = St_{max}/St_0$ on the edge surface at these flow conditions ($M_\infty = 6,5$; $Re_\infty = 10^5 + 10^6$).

As the Reynolds number decreases, when the shock layer becomes fully viscous and, consequently, shocks and mixing layer boundaries become smeared, extreme values of heat fluxes to the edge decrease, and the type IV interference, featured by

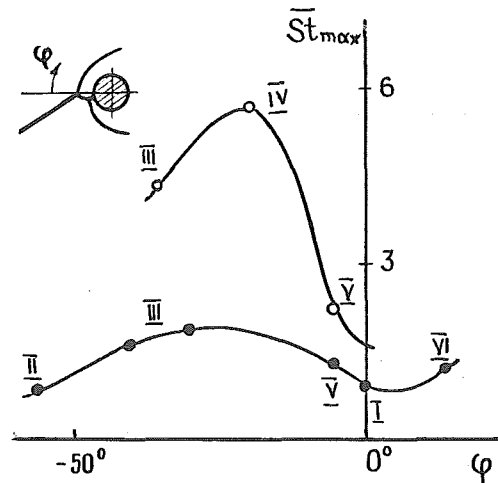


Figure 8. Maximal Heat Flux Distribution for Different Types of Interference on a Cylinder

greatest values of St_{max} , is not realized. Such kind of information is given in Fig.8 for $M_\infty = 6,5$ and $Re_\infty \approx 10^2$.

Many local simulation problems require increased characteristic dimensions of test models. In some cases this difficulty is overcome owing to the use of unique measuring device possibilities.

An example of this kind of investigations using special discrete transducers is presented in [8] for the case of the measurement of heat flux on the surface of a protruding or a recessed tile. In other cases, the characteristic dimension of the flow under investigation can be increased considerably due to a reduction in density in vacuum wind tunnel tests.

The formation of low density flows with known properties characterizing the flow in the region under study is more promising. In case of a hypersonic flow over a vehicle, the problem of a local simulation of a flow near its surface is reduced to the respective problem of a subsonic low-density gas flow. The possibilities of increasing the flow scale are very great here. In [15], e.g., this increase in the experiment was brought up to the characteristic dimensions of Knudsen layer ($L \approx \lambda$), where a velocity profile was measured.

At $\lambda \ll L$, the local simulation transits to the region of continuum flow condition. In this case, a laminar flow with a specified vorticity near the streamlined body surface will correspond to the wall boundary layer region flow. The effect of increasing flow scale here can be used to study the influence of small disturbances on boundary layer flow, separation zone initiation, etc.

For the solution of these problems in an experiment at low pressures, a technique has been developed to obtain subsonic low-density flows with specified vorticity distribution using porous media. The ways of developing this method in aerodynamic experiment at low Reynolds numbers are considered in [16].

The subsonic low-density flows obtained by using porous media were used in aerodynamic experiment for a local simulation of a hypersonic flow in the stagnation point vicinity. The effect of an increased flow scale was used for the determinati-

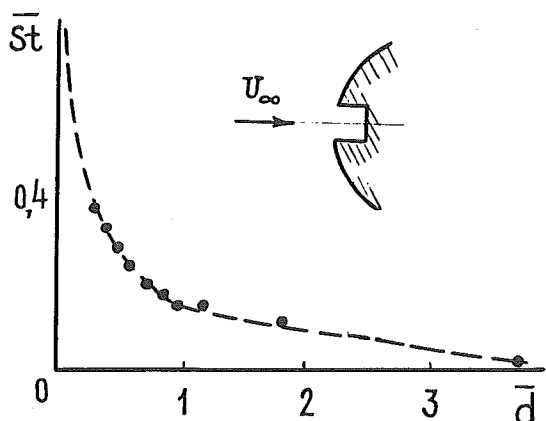


Figure 9. Heat Transfer At The Recess Bottom

on of heat transfer at the body stagnation point in the presence of a cylindrical recess or rectangular grooves. The measurement results are given in fig. 9, where a relative variation in heat transfer \overline{St} at the recess bottom is shown depending on its relative depth $d = d/D$. The data obtained for heat transfer coefficient in the vicinity of stagnation point in the presence of roughnesses

on its surface can be extended to a hypersonic flow. In the above considered case, from local simulation conditions it follows that $Re_0 = 76,5$.

Obviously, it will be impossible to obtain similar evidence for this flow condition in hypersonic wind tunnels because of small model dimensions.

Concluding Remarks

The above considered principles of simulation and the abundant information on hypersonic body flow peculiarities from continuum to free-molecular flow conditions accumulated by now is widely used for the determination of aerodynamic and thermal characteristics of hypersonic vehicles. Many of these results formed the application program "Vysota" ("Altitude") that comprises the computation of aerodynamic and thermal characteristics of hypersonic vehicles including those with skeleton-net elements, the calculation of heat-stressed vehicle components, the systematization of the results of the laboratory study of hypersonic flow - various coating materials interaction laws, the flow parameters calculation in a disturbed flow field in the conditions of mass evaporation, the evaluation of errors of different methods. The system program package part includes effective and simple ways of forming the geometry of a vehicle, the methods of its control, including visualization, and high-quality storage and information processing techniques.

References

1. Zhilin Yu.L. "Similarity Parameters at High Hypersonic Velocities", *Prikladnaya matematika i mehanika (PMM)*, v. XXVI, issue 2, 1962 (in Russian).
2. Gusev V.N., Kogan M.N., Perepukhov V.A. "On Similarity and Variation of Aerodynamic Characteristics in Transition Region at Hypersonic Flow Velocities", *Uchenye Zapiski TsAGI (Scientific Notes of TsAGI)*, v.1, N1, 1970 (in Russian).
3. Gusev V.N., Yerofeyev A.J., Klimova T.V., Perepukhov V.A., Ryabov V.V., Tolstykh A.J. "Theoretical and Experimental Investigations of Hypersonic Rarefied Gas Flows Over Simple Shape Bodies", *Proceedings of TsAGI*, issue 1855, 1977 (in Russian).
4. Kogan M.N. "Rarefied Gas Dynamics", Nauka Publishers, 1967 (in Russian).
5. Nikolayev V.S. "Approximation Formulae for Local Aerodynamic Characteristics of Wing-Type Bodies in a Viscous Hypersonic Flow over a Wide Range of Similarity Parameters", *Uchenye Zapiski TsAGI (Scientific Notes of TsAGI)*, v. XII, N4, 1981 (in Russian).
6. Gorenbukh P.I. "On Approximate Calculation of Aerodynamic Characteristics of Simple Bodies in a Hypersonic Rarefied Gas Flow", *Proceedings of TsAGI*, issue 2436, 1990 (in Russian).

7. Blanchard R.C., Buck G.M. "Determination of Rarefied Flow Aerodynamics of the Shuttle Orbiter from Flight Measurements on STS-6 and STS-7", AIAA Paper 85-0347, 1985.
8. Lozino-Lozinsky G.E., Neiland V.Ya. "The Convergence of the Buran Orbiter Flight Test and Preflight Study Results and the Choice of Strategy to Develop a Second-Generation Orbiter", AIAA Paper 89-5019, 1989.
9. Blanchard R.C., Larman K.T. "Rarefied Aerodynamics and Upper Atmosphere Flight Results from the Orbiter High Resolution Accelerometer Package Experiment", AIAA Paper 87-2366, 1987
10. Gusev V.N. "The Investigation of the Hypersonic Vehicle Aerothermodynamics", AIAA Paper 90-5271, 1990.
11. Perminov V.D., Gorelov S.L., Freedlander O.G., Khmelnitsky A.A. "Approximate Aerodynamic Analysis for Complicated Bodies in Rarefied Gas Flow", - Proc. of the 17th Int. Symp. on RGD Aachen, 1990.
12. Gusev V.N., Provotorov V.P. "Simulation of Altitude Flight Full-Scale Conditions in Wind Tunnels", Uchenye Zapiski TsAGI (Scientific Notes of TsAGI), v.XIII, N3, 1982 (in Russian)
13. Botin A.V., Gusev V.N., Provotorov V.P. "Hypersonic Flow over Blunt Edges at Low Reynolds Numbers", Prikladnaya mehanika i tekhnicheskaya fizika (PMTF), N4, 1989 (in Russian).
14. Wieting A.R., Holden M.S. "Experimental Shock-Wave Interference Heating on a Cylinder at Mach 6 and 8", AIAA Journal, v.27, N11, 1989.
15. Reynolds M.A., Smolderen J.I., Wendt J.F. "Velocity Profile Measurements in the Knudsen Layer for Kramers Problem", Proc. of the 9th Int. Symp. on RGD, Göttingen, 1974
16. Gusev V.N., Nikolsky Yu.V. "Porous Media in Aerodynamic Test at Low Reynolds Number", Proc. of the 13th Int. Symp. on RGD, Novosibirsk, 1982.